J|A|C|S
ARTICLES
Published on Web 08/07/2002

Molecule-Based Room-Temperature Magnets: Catalytic Role of V(III) in the Synthesis of Vanadium−Chromium Prussian Blue Analogues

Raquel Garde,[†] Françoise Villain,[†,‡] and Michel Verdaguer*[,†]

Contribution from the Laboratoire de chimie inorganique et matériaux moléculaires, Unité associée au C.N.R.S. 7071, Université Pierre et Marie Curie, 75252 Paris Cedex 05, France, and Laboratoire pour l'Utilisation du Rayonnement Electromagnétique, Bât 209D, Centre Universitaire - B.P. 34 - 91898 Orsay Cedex, France

Received April 11, 2002

Abstract: A new synthetic procedure to obtain vanadium−chromium Prussian blue analogues is presented, using controlled amounts of V^{III} in solution during the synthesis. The vanadium and chromium oxidation states and the chemical environment of the metal ions in the solids are characterized by infrared and X-ray absorption spectroscopies. The presence of weak amounts of V^{III} during the synthesis provides materials which are better organized and present reproducible Curie temperature and magnetization at saturation in agreement with the observed V/Cr stoichiometry.

Introduction

The synthesis of materials with new and predictable properties is a challenge for chemists. A few years ago, inorganic molecular chemists were engaged in the synthesis of high-temperature molecule-based magnets, and this area remains very active.[1] In 1991, looking for charge-transfer vanadium-based molecular materials, Manriquez et al. synthesized the first molecule-based magnet with a Curie temperature (T_C) above room temperature ($V[TCNE]_x \cdot yCH_2Cl_2$ ($x \approx 2$, $y \approx 0.5$, TCNE = tetracyanoethylene)).[2] However, the compound decomposes before reaching T_C, and until today it was not fully characterized. [3]

Some years later, in 1995, a molecule-based Prussian blue analogue made from hexacyanochromate(III) and vanadium(II) $V[Cr(CN)_6]_{0.86} \cdot 2.8\ H_2O$ was claimed to present a Curie temperature $T_C = 315$ K, and its synthesis was based on a rational approach.[4] In a comment, Kahn[5] underlined that, on one hand, "*the synthesis of such a material can be considered as a cornerstone in the field of molecular magnetism*" ... and that $V[Cr(CN)_6]_{0.86} \cdot 2.8\ H_2O$ was "*an excellent example on which to learn (or to teach) the basic concepts of molecular magnetism*". On the other hand, Kahn pointed out that it "*is not a molecular compound, but rather an amorphous and nonstoichiometric compound*", "*the saturation magnetization is limited to 0.15 Bohr magnetons ...*", "*the coercive field is only 10 Oe...*"

Indeed, these nonstoichiometric vanadium chromium Prussian blue analogues build a wide family which can be formulated as $A_x^- C_y^+ V^{II}_{\alpha} V^{III}_{(1-\alpha)}[Cr(CN)_6]_z \cdot y$(solvent) (A, anion; C, cation). Amorphous or badly crystallized, the samples often contain uncontrolled amounts of vanadium(III). Thus, a wide field of investigation remained open for chemists to further improve the structural and magnetic properties of the compound.[1a,4,6−11] Following analogous recipes and the same reactants, Miller et al. were able to push the Curie temperature up to 373 K.[6] Girolami et al.[7] used a sol−gel approach, modified the stoichiometry, and succeeded in obtaining a $T_C = 376$ K, that is, above the boiling temperature of water. In both cases, the structure is not fully defined (even if Girolami provided powder X-ray diffraction data), the magnetization at saturation remains far from that expected from stoichiometry, and, moreover, the Curie

* To whom correspondence should be addressed. E-mail: miv@ccr.jussieu.fr.
[†] Université Pierre et Marie Curie.
[‡] Centre Universitaire.

(1) (a) Verdaguer, M.; Bleuzen, A.; Train, C.; Garde, R.; Fabrizi de Biani, F.; Desplanches, C. *Philos. Trans. A* **1999**, *357*, 2959−2976. (b) Verdaguer, M.; Bleuzen, A.; Marvaud, V.; Vaissermann, J.; Seuleiman, M.; Desplanches, C.; Sciuller, A.; Train, C.; Garde, R.; Gelly, G.; Lomenech, C.; Rosenman, I.; Veillet, P.; Cartier dit Moulin, C.; Villain, F. *Coord. Chem. Rev.* **1999**, *190*, 1023−1047. (c) Miller, J. S.; Epstein, A. J. *MRS Bull.* **2000**, *25* (11), 21−71. (d) *Polyhedron*; Christou, G., Ed.; 2001; Vol. 20, Issues 11−14. (e) Verdaguer, M.; Gatteschi, D.; Day, P. *L'Actualité Chim.* **2001**, 6.
(2) Manriquez, J. M.; Yee, G. T.; McLean, R. S.; Epstein, A. J.; Miller, J. S. *Science* **1991**, *252*, 1415−1417.
(3) Gordon, D. C.; Deakin, L.; Atta, M. A.; Miller, J. S. *J. Am. Chem. Soc.* **2000**, *122*, 290.
(4) Ferlay, S.; Mallah, T.; Ouahès, R.; Veillet, P.; Verdaguer, M. *Nature* **1995**, *378*, 701−703.
(5) Kahn, O. *Nature* **1995**, *378*, 667−668.
(6) Hatlevik, O.; Buschmann, W. E.; Zhang, J.; Manson, J. L.; Miller, J. S. *Adv. Mater.* **1999**, *11*, 914−918.
(7) Holmes, S. M.; Girolami, S. G. *J. Am. Chem. Soc.* **1999**, *121*, 5593−5594.
(8) Dujardin, E.; Ferlay, S.; Phan, X.; Desplanches, C.; Cartier dit Moulin, C.; Sainctavit, P.; Baudelet, F.; Dartyge, E.; Veillet, P.; Verdaguer, M. *J. Am. Chem. Soc.* **1998**, *120*, 11347−11352.
(9) Garde, R.; Desplanches, C.; Bleuzen, A.; Veillet, P.; Verdaguer, M. *Mol. Cryst. Liq. Cryst.* **1999**, *333A*, 587.
(10) Verdaguer, M.; Bleuzen, A.; Marvaud, V.; Vaissermann, J.; Tournilhac, F.; Train, C.; Ouahès, R.; Garde, R.; Fabrizi de Biani, F.; Desplanches, C.; Sciuller, A. In *Coordination Chemistry at the Turn of the Century*; Ondrejovic, G., Sirota, A., Eds.; Slovak Technical University Press: Bratislava, 1999; Vol. 4, p 67.
(11) Ferlay, S.; Mallah, T.; Ouahès, R.; Veillet, P.; Verdaguer, M. *Inorg. Chem.* **1999**, *38*, 229−234.

temperature decreases after one thermal cycle around the T_C. Hashimoto and Desplanches were able to produce high T_C electrochromic thin films of VCr.[12,13] An amazing case, with a lower T_C (~310 K) but improved magnetization at saturation, is the one of two samples which present close macroscopic properties but opposite local magnetization on the two paramagnetic chromium and vanadium centers.[8] Moreover, the VCr derivatives are air-sensitive and change their magnetic properties more or less rapidly when left in air.

In a systematic step to better control the properties of such compounds, as others, we experienced that the oxidation state and the electronic structure of the vanadium, the stoichiometry, and the crystallinity of the precipitate are important parameters to determine the magnetic properties.[1,4,6−10] During our studies, we discovered that (a) in a perfect anaerobic atmosphere, the slowly precipitating solid is no longer a room-temperature magnet, and (b) some oxidation of the vanadium ion during the synthesis is necessary to reach a Curie temperature above ambient. Both observations prompted us to look more closely at the role of vanadium(III) during the synthesis.

The present paper is dedicated to vanadium−chromium (VCr) Prussian blue derivatives with $V_1Cr_{2/3}$ stoichiometry (sometimes formulated as $V_4Cr_{8/3}$ or V_3Cr_2). We show that the presence of small amounts of V(III) during the synthesis is a key factor to get such systems presenting high T_C, reproducible magnetic properties, and magnetization at saturation consistent with the stoichiometry.

Experimental Section

Synthesis. Starting Materials. $K_3[Cr(CN)_6]$ was obtained as already described.[11] $(TBA)_3[Cr(CN)_6]$ (TBA = $[N(^nBu)_4]^+$) is obtained by mixing aqueous solutions of $K_3[Cr(CN)_6]$ and TBABr. The precipitate is purified by dissolution in ethanol and precipitation with ethyl ether (Et_2O). The IR spectrum displays a unique strong $\nu_{as}C{\equiv}N$ stretching band centered at 2110 cm^{-1}. The synthesis of the Tutton salt and $[V(MeOH)_6]I_2$ (MeOH = methanol) was carried out as already described.[14,15] All of the reactions leading to the synthesis of the VCr derivatives were carried out in a glovebox.

Compound $V[Cr(CN)_6]_{0.65}(I)_{0.05}{\cdot}4H_2O$, **1**, was obtained by mixing aqueous solutions of $(TBA)_3[Cr(CN)_6]$ (0.627 g, 6.7×10^{-4} mol) and $[V(MeOH)_6]I_2$ (0.5 g, 1×10^{-3} mol, 0.05 mol L^{-1}). A deep blue solid precipitated immediately. We left the suspension for 1 day. To recover the compound, which was difficult to filter, we evaporated to dryness, we washed the solid with 50 mL of H_2O and 30 mL of ethanol (EtOH), and we dried it under vacuum during 2 h (procedure 1).

Anal. Found (Calcd): 17.57% (17.63%) C; 3.61% (3.07%) H; 16.16% (20.56%) N; 2.26% (2.27%) I; 12.70% (12.72%) Cr; 19.35% (19.39%) V. IR (broad): 2110 cm^{-1}. T_C: 260 K.

Compound $V[Cr(CN)_6]_{0.67}(TBAI)_{0.012}{\cdot}5H_2O$ 1.44EtOH, **2**, was obtained by mixing aqueous solutions of $(TBA)_3[Cr(CN)_6]$ (0.627 g, 6.7×10^{-4} mol), $[V(MeOH)_6]I_2$ (0.5 g, 1×10^{-3} mol, 0.05 mol L^{-1}), and 2.5% of V(III) (VCl_3) [%V(III) = mol of V(III)/100 mol of V(II)]. A deep blue solid precipitated immediately. We left the suspension for 1 day, and, as the particle size was large enough, we filtered without evaporation. The solid was washed with 50 mL of H_2O and 30 mL of EtOH and dried under vacuum during 2 h (procedure 2).

Anal. Found (Calcd): 24.14% (24.25%) C; 4.32% (5.47%) H; 18.22% (16.08%) N; 0.44% (0.43%) I; 9.90% (9.92%) Cr; 14.50% (14.50%) V. IR (narrow): 2116 cm^{-1}. T_C: 310 K.

We prepared 23 compounds following procedure 1 or 2, in the presence of different amounts of V(III) during the synthesis. After separation of the precipitate, we checked the presence of V(III) in the filtrate by electronic spectroscopy. Some of the 23 compounds were prepared using a V(II)/$[Cr(CN)_6]$ ratio smaller than $^3/_2$ during the synthesis. All of the derivatives prepared with an amount of V(III) in solution between 1 and 20% present a stoichiometry close to the ideal $V_1Cr_{2/3}$ one, whatever the percentage of V(III) during the synthesis. In most cases, the experimental nitrogen analysis is different from the calculated one. This systematic deviation, already experienced by other groups engaged in Prussian blues analogues chemistry,[7] appears intrinsic to the elementary analysis technique applied to Prussian blues.

Electronic Spectroscopy. The electronic spectra of aqueous solutions of the different compounds and the kinetic studies were recorded at room temperature under argon atmosphere on a SHIMADZU UV-2101PC UV−visible spectrophotometer in the 300−900 nm range.

Magnetic Measurements. The T_C's of all of the compounds were determined by permeability measurements.[16] The magnetization measurements were performed with a Quantum Design SQUID magnetometer in the 4−400 K temperature range in a 200 Oe applied magnetic field.

Infrared Spectroscopy. The infrared spectra were recorded under inert atmosphere using a Bio-Rad FTIR spectrophotometer, in the 4000−400 cm^{-1} range with KBr pellets containing 1% in mass of the sample.

X-ray Absorption Spectroscopy (XAS). XAS experiments were performed on the XAS 13 beam line at the French synchrotron facility DCI at LURE (Orsay). Spectra were recorded at the vanadium and chromium K-edges in transmission mode using Si 311 (XANES) and Si 111 (EXAFS) double monochromator detuned around 30% to ensure harmonic rejection. For the edge spectra, we recorded simultaneously the spectra of the samples and that of a vanadium or chromium foil with a third ionization chamber to check energy calibration. The edge energies of the vanadium (5465 eV) and the chromium (5989 eV) were fixed at the first inflection point of the metallic foils. The samples were ground and homogeneously dispersed in cellulose pellets in a glovebox and kept in an anaerobic chamber under helium atmosphere during the measurements.

Edge spectra were recorded with 0.3 eV steps with an integration time equal to 2 s per point. The spectra were normalized at the middle of the first EXAFS oscillation. EXAFS spectra were recorded using 2 eV steps. The two first steps of the EXAFS signal treatment were performed with the "EXAFS pour le Mac" code.[17] The EXAFS signal was extracted from the data by subtracting a linear preedge background, a combination of polynomials and cubic spline atomic absorption background, and was normalized by the Lengeler−Eisenberger procedure.[18] The pseudoradial distribution function was given by the Fourier transform (FT) of $w(k)k^3\chi(k)$, where $w(k)$ is a Kaiser−Bessel window with a smoothness parameter equal to 3 (k is the wavenumber). At the vanadium K-edge, the k range is limited to 2.0−11.2 $Å^{-1}$ (Δk = 9.2 $Å^{-1}$), due to the presence of the chromium edge. At the chromium K-edge, the k limits are equal to 2.5−13.1 $Å^{-1}$ (Δk = 10.6 $Å^{-1}$). In Prussian blue analogues, the multiple scattering is expected to be important, due to the alignment V−N−C−Cr. The EXAFS signal simulation in a single scattering mode is not feasible. Therefore, the quantitative analysis (number of neighbors, distances, Debye−Waller factor) used the FEFF7 code[19] and multiple scattering.

(12) Ohkoshi, S.; Mizuno, M.; Hung, G.; Hashimoto, K. *J. Phys. Chem. B* **2000**, *104*, 9365−9367.
(13) Desplanches, C. PhD Thesis, Université Pierre et Marie Curie, Paris, 2001.
(14) Larkworthy, L. F.; Murphy, J. M.; Patel, K. C.; Phillips, D. J. *J. Chem. Soc. A* **1968**, 2936−2938.
(15) Larkworthy, L. F.; O'Donoghue, M. W. *Inorg. Chim. Acta* **1983**, *71*, 81−86.
(16) Tournilhac, F. G.; Garde, R.; Verdaguer, M. *Inorg. Chim. Acta* **2001**, *326*, 73−77.
(17) Michalowicz, A. In *EXAFS pour le MAC*; Logiciels pour la Chimie, Ed.; Société Française de Chimie: Paris, 1991; p 102.
(18) Lengeler, B.; Eisenberger, P. *Phys. Rev. B* **1980**, *21*, 4507.
(19) Zabinsky, S. I.; Rehr, J. J.; Ankudinov, J. J.; Albers, R. C.; Eller, M. J. *Phys. Rev.* **1995**, *B52*, 2995.

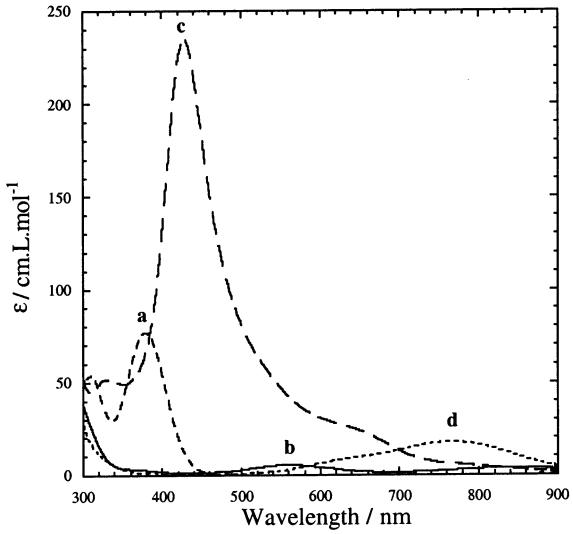

Figure 1. Electronic spectra (molar absorption coefficient) of solutions: (a) $(TBA)_3[Cr(CN)_6]$ (0.033 mol L^{-1}), (b) $[V(MeOH)_6]I_2$ (0.05 mol L^{-1}), (c) $V(SO_3CF_3)_3$ (0.01 mol L^{-1}), and (d) $VOSO_4 \cdot 5H_2O$ (0.05 mol L^{-1}).

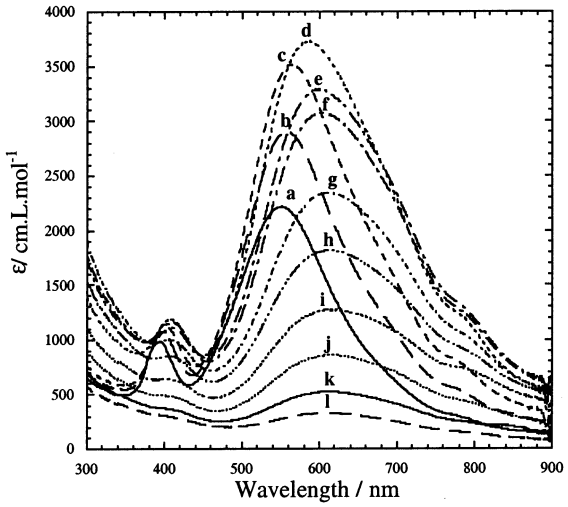

Figure 2. Changes as a function of time of the spectrum (molar absorption coefficient relative to vanadium) of a solution mixture of $[V(MeOH)_6]I_2$ (5×10^{-4} mol L^{-1}) and $(TBA)_3[Cr(CN)_6]$ (3.3×10^{-4} mol L^{-1}) at (a) 5, (b) 15, (c) 25, (d) 40, (e) 45, (f) 55, (g) 65, (h) 95, (i) 105, (j) 115, (k) 155, and (l) 195 min.

Results

Electronic Spectroscopy. In Figure 1 are shown the electronic spectra of V(II) (0.05 mol L^{-1}), V(III) (0.01 mol L^{-1}), V(IV) (0.05 mol L^{-1}), and $[Cr(CN)_6]^{3-}$ (0.033 mol L^{-1}) aqueous solutions. We checked that under slow diffusion of dioxygen in a V(II) solution, V(II) is oxidized to V(III); we did not observe in such conditions the presence of VO^{2+} (aq). The electronic spectrum of the V(II) aqueous solution shows two maxima at 850, 560 [$^4A_{2g} \rightarrow {}^4T_{2g}$, $^4A_{2g} \rightarrow {}^4T_{1g}$(F) transitions] and a weak shoulder at 320 nm [$^4A_{2g} \rightarrow {}^4T_{1g}$(P)]. The band at 380 nm corresponds to a forbidden transition. The electronic spectrum of the V(III) aqueous solution displays three maxima at 650, 425, and 327 nm [$^3T_{1g} \rightarrow {}^3T_{2g}$ and $^3T_{1g} \rightarrow {}^3A_{2g}$ and $^3T_{1g} \rightarrow {}^3T_{1g}$(P) transitions]. The spectrum of the VO^{2+} aqueous solution presents two maxima at 768 and 620 nm [$^2B_2 \rightarrow {}^2E$ and $^2B_2 \rightarrow {}^2B_1$ transitions]. Finally, the electronic spectrum of $(TBA)_3[Cr(CN)_6]$ shows two maxima at 390 and 320 nm corresponding to the $^4A_{2g} \rightarrow {}^4T_{2g}$ and $^4A_{2g} \rightarrow {}^4T_{1g}$(F) transitions.

We carried out kinetic studies of the synthetic reaction by mixing V(II) (5×10^{-4} mol L^{-1}) and $[Cr(CN)_6]^{3-}$ (3.3×10^{-4} mol L^{-1}) aqueous solutions ($V_1/Cr_{2/3}$ ratio). Figure 2 displays the changes in the electronic spectra of the mixture when the reaction proceeds. The three bands with maxima at 393, 550, and 790 nm shift to higher wavelengths. They reach an absorbance maximum after 40 min of reaction, and then their absorbance decreases slowly. At this point, the beginning of the precipitation of a blue solid can be observed. The band at 800 nm can be assigned to a forbidden transition for $[Cr(CN)_6]^{3-}$ that becomes allowed when coordinated to V(II). The intense band at 550 nm can be safely assigned to a V(II)−NC−Cr charge transfer. The shift of the maxima to a higher wavelength is frequent for the formation of aggregates.

We carried out the study of the change in the electronic spectrum of a $V(III)(SO_3CF_3)_3$ (3×10^{-3} mol L^{-1}) and $K_3[Cr(CN)_6]$ (3×10^{-3} mol L^{-1}) mixture solution. Three bands are observed at 440, 650, and ~800 nm. The absorbance increases with time. The maximum of the band at 650 nm shifts to a higher wavelength, whereas the two bands at 440 and 800 nm remain at the same energy. After 120 min, a suspension of a green-blue solid appears. After 210 min, a solid precipitates, and the absorbance decreases. A new band appears at 350 nm, and the band at 440 nm shifts to 460 nm. When the reaction proceeds in the presence of V(III), it is not possible to determine the spectroscopic differences because the molar absorption coefficients ϵ of the V(II)/chromicyanide solution are much higher (by a factor 15) than that of the V(III)/chromicyanide solution; it can be observed, nevertheless, that the precipitate occurs much more rapidly.

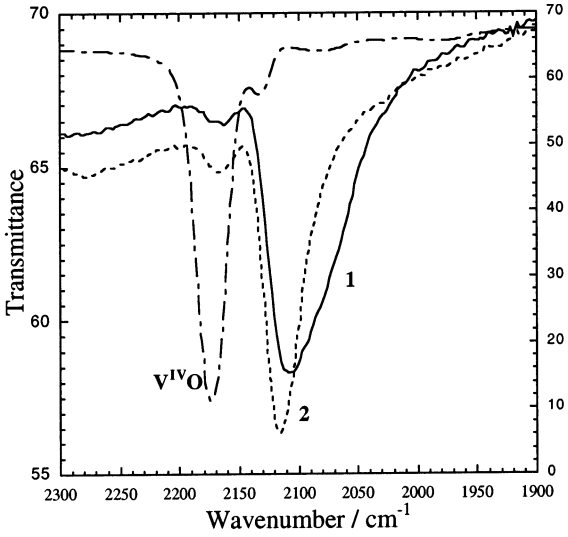

Figure 3. Infrared spectra of **1** (−), **2** (− − −), and $(VO)_3[Cr(CN)_6]_2$ (− · − · −).

IR Spectroscopy. In Figure 3 are shown the IR spectra of compounds **1** (V(II), obtained without V(III) during the synthesis), **2** (obtained in the presence of 2.5% V(III) during the synthesis), and their vanadyl $V^{IV}O$ analogue $(VO)_3[Cr(CN)_6]_2$ in the 1900−2300 cm^{-1} range. In this part of the IR spectrum appear the $\nu_{as}C{\equiv}N$ asymmetric stretching bands, which are sensitive to the bonding mode of the cyanide and to the oxidation state of the metallic ions coordinated to the CN bridge. For **1**, a broad band at 2110 cm^{-1} can be assigned to V(II)−N≡C−Cr(III) sequences. It presents several shoulders

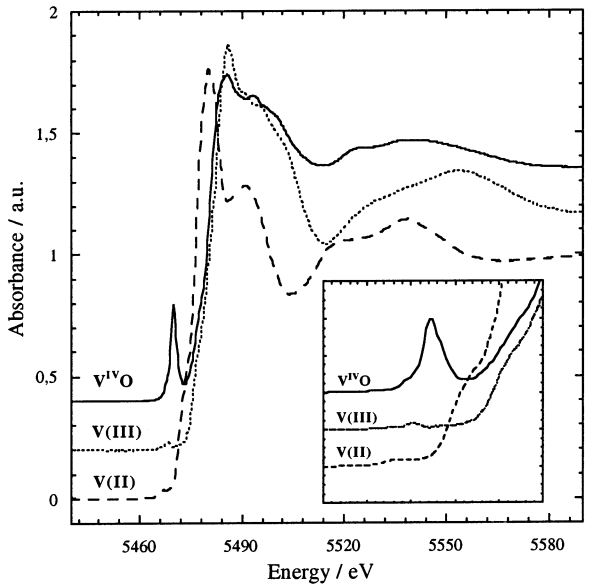

Figure 4. Vanadium K-edge spectra of the models $(NH_4)_2V^{II}(SO_4)_2 \cdot 6H_2O$ (− − −), $V^{III}(SO_2CF_3)_3$ (···), and $V^{IV}OSO_4 \cdot 5H_2O$ (—). 0.2 and 0.4 in absorbance for clarity shift the spectra.

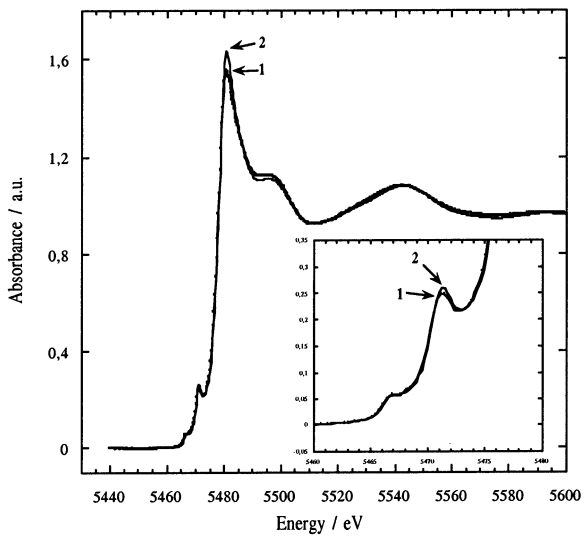

Figure 5. Vanadium K-edge spectra in **1** (−•−) and **2** (−).

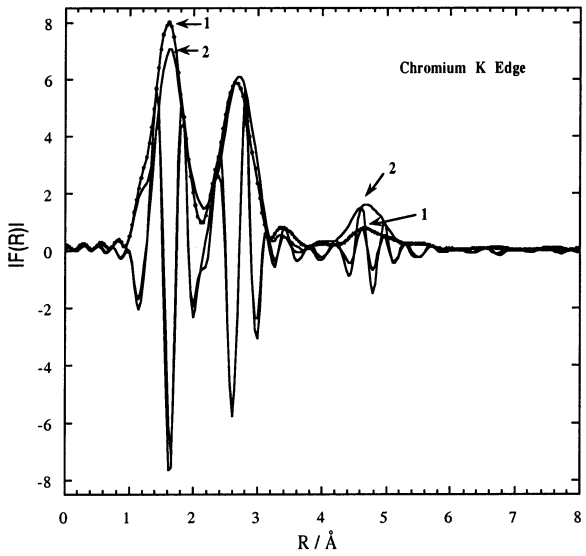

Figure 6. Fourier transform moduli and imaginary part of the EXAFS signal at the chromium K-edge for **1** (−•−) and **2** (−).

on the low wavenumbers side. For **2**, there are two bands, one band of strong intensity centered at 2116 cm^{-1}, corresponding to a V(II)−N≡C−Cr(III) sequence, and another very weak one, centered at 2165 cm^{-1}, assigned to a $V^{IV}O$−N≡C−Cr(III) sequence. (NB: The pure vanadyl derivative displays only one narrow, intense band centered at 2175 cm^{-1} ($V^{IV}O$−N≡C−Cr(III) sequence) and the very intense band at 981 cm^{-1} corresponding to the $\nu_{as}V^{IV}$═O stretching.[8,11,20]) For compound **2**, obtained in the presence of V(III) during the synthesis, the nonobservation of the V^{IV}═O stretching band at 981 cm^{-1} is consistent with a tiny amount of vanadyl in the compound. Under exposure to air of **1** and **2**, we observed the slow appearance of the two bands at 2175 cm^{-1} [$V^{IV}O$−N≡C−Cr(III)] and at 981 cm^{-1}, signature of the presence of vanadyl.

X-ray Absorption Spectroscopy. In Figure 4 are presented the XANES spectra of three reference compounds, $(NH_4)_2V(II)(SO_4)_2 \cdot 6H_2O$, $V(III)(SO_2CF_3)_3$, and $V^{IV}OSO_4 \cdot 5H_2O$. The preedge spectra of the models display one peak of weak intensity at 5466.6 eV for V(II) and at 5468.2 eV for V(III) and one intense peak at 5469.8 eV for $V^{IV}O$. In this energy range are observed 1s to 3d transitions, forbidden in octahedral complexes [V(II) and V(III)] and partially allowed in square pyramidal ones [$V^{IV}O$]. The edge energy positions ("white line", corresponding to the maximum of the edge) are 5480.3, 5485.8, and 5485.6 eV for V(II), V(III), and $V^{IV}O$, respectively. This energy range corresponds to allowed transitions to the p-symmetry orbitals.

The XANES spectra of the reference compounds allow us to characterize the different oxidation degrees of vanadium in compounds **1** and **2**. In Figure 5 are displayed the vanadium K-edge spectra for **1** and **2**. The preedge shows a weak band at 5466.6 eV [assigned to octahedral V(II)] and one band at 5471.2 eV which corresponds to an allowed transition from 1s to t_{1u} symmetry molecular orbitals, a combination of p orbitals of the vanadium and π^* cyanide orbitals, as shown previously.[8] In vanadium−chromium Prussian blue analogues, this band is a signature of the interaction between V(II) and NC−Cr(III).[8] There is no band at 5468.2 eV, which shows the absence of V(III). The top of the edge energy is 5481 eV, much closer to that of the V(II) reference than to that of V(III). The edge is more intense for **2** than for **1**. For a quasi-octahedral surrounding, the higher and narrower this peak is (due to the degeneracy of p orbitals), the closer to an octahedron the structure around the metal is. Everything being equal, the intensity of the 5471.2 eV peak is inversely correlated to the intensity of the white line (because the more the p metal orbitals are engaged in the π^* MOs, the less they are available for other orbitals). The peak at 5471.2 eV is observed for both compounds, more intense for **2** than for **1**.

At the chromium K-edge, the spectra are very similar in the two compounds and close to that of the $K_3[Cr(CN)_6]$ precursor.

We first give qualitative observations at the chromium and vanadium edge before entering in the quantitative analysis.

At the chromium K-edge, for compounds **1** and **2**, the Fourier transforms of the EXAFS signal (Figure 6) display three peaks assigned to the three shells around the chromium. The two first

(20) Nakamoto, K. *Infrared and Raman Spectra of Inorganic and Coordination Compounds*; J. Wiley and Sons: New York, 1978.

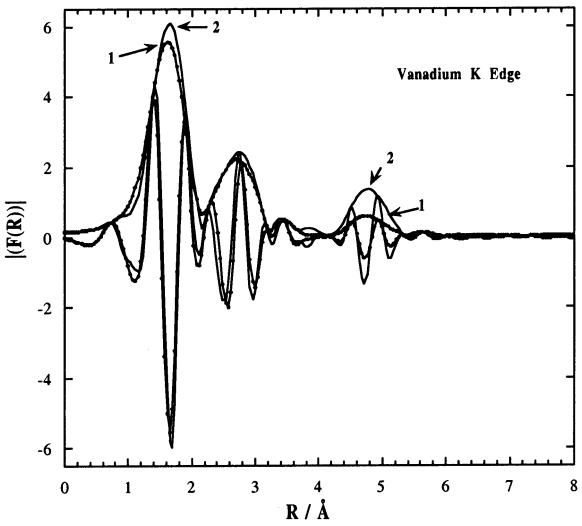

Figure 7. Fourier transform moduli and imaginary parts of the EXAFS signal at the vanadium K-edge for **1** (−•−) and **2** (−).

shells correspond to the carbon and nitrogen atoms of the cyanide ligand. The third shell corresponds to heavy neighbors, the vanadium ions.

The first and second peaks are very similar in intensities (modulus) and distances (imaginary part) for both compounds and for the $K_3Cr(CN)_6$ precursor. The strong difference is observed in the intensity in the third peak that is more intense for **2** than for **1**. The Cr−V distance in **2** (from imaginary part) appears slightly longer than in **1**. The observation that the first and second shells are identical can be considered as trivial information. For such poorly crystalline compounds, it is the confirmation of the molecule-based nature of the samples: the $[Cr(CN)_6]^{3-}$ molecular precursor is indeed a building block of the solid, kept unchanged.

At the vanadium K-edge, for compounds **1** and **2**, the Fourier transforms of the EXAFS signals of both compounds (Figure 7) also display three peaks attributed to three shells of neighbors. The first peak of the Fourier transform corresponds to two subshells: nitrogen neighbors (V−N, from cyanide) and oxygen ones (V−O, from coordinated water), according to the stoichiometry $V_1Cr_{2/3}$. The second peak corresponds to the carbon atom of the cyanide ligand, and the third one corresponds to the chromium atoms. The intensities of the peaks corresponding to the first and second shells of **1** and **2** are not so different, but the third peak is more intense in **2** than in **1**. From the imaginary parts of the spectra, we observe that in the first shell, the mean distances appear slightly shorter in **1** than in **2**, whereas in the second shell the opposite becomes true.

The quantitative analysis of the EXAFS is not easy because of the presence of (i) multiple scattering effects in the second and third shells signals originating in the more or less linear V−N≡C−Cr units and (ii) possible different V−N≡C−Cr bridges. To extract information about the distances, their distribution (Debye−Waller factor), and the bond angles around the metallic atoms, we therefore modeled the EXAFS signal using the FEFF7 code.[19] For compound **2**, at the vanadium K-edge, we computed the EXAFS signal using multiple scattering in the following model gathering previously known information (Scheme 1): two V−O units at a distance of 2.06 Å,[4,11] four V−N≡C−Cr units with various V−N−C angles, a 180° N−C−Cr angle, a 2.12 Å V−N distance, a 1.15 Å N−C distance, and a 2.06 Å C−Cr distance.[4,11] The structural parameters in better agreement with the experimental data correspond to a 168° V−N−C angle and are given in Table 1.

Scheme 1

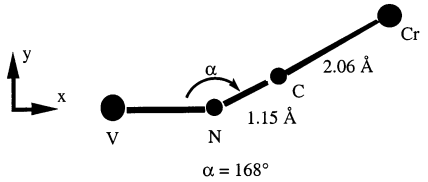

Table 1. Structural Parameters at the Vanadium K-Edge for Compounds **1** and **2**

neighbors	N^a	R^b/Å in **1**	R^b/Å in **2**	σ^c/Å in **1**	σ^c/Å in **2**
N (O)	4 (2)	2.14 (2.05)	2.12 (2.06)	0.12 (0.05)	0.09 (0.05)
C	4	3.27	3.24	0.09	0.09
Cr	4	5.31	5.27	0.13	0.10

[a] *N*, number of neighbors around vanadium. [b] Vanadium−neighbors distance. [c] Debye−Waller factor.

Table 2. Structural Parameters at the Chromium K-Edge for Compounds **1** and **2**

neighbors	N^a	R^b/Å in **1** and **2**	σ^c/Å in **1**	σ^c/Å in **2**
C	6	2.06	0.05	0.06
N	6	3.21	0.08	0.08
V	6	5.31 (**1**), 5.27 (**2**)	0.13	0.10

[a] *N*, number of neighbors around chromium. [b] Chromium−neighbors distance. [c] Debye−Waller factor.

For compound **1**, we followed the same analysis scheme taking into account two observations: (i) the observed mean distance of the first shell in **1** is slightly shorter than that in **2**, and (ii) the distance of the second shell in **1** is longer than that in **2**. The model was modified as follows (see Table 1): in the first shell, the two V−O distances become shorter, 2.05 Å, with a smaller Debye−Waller factor, and the four V−N distances becomes longer, 2.14 Å, with a larger Debye−Waller factor than for **2**. We fixed $\alpha = 168°$ as in **2**. The parameters, which better reproduce the experimental data, are collected in Table 1. The Debye−Waller factor for the third shell (Cr atoms) is large.

At the chromium K-edge, we used exactly the same models as above for **1** and **2**, and we calculated the EXAFS signal for six Cr−C≡N−V units, only changing the Debye−Waller factors and taking the N−V distance in **1** as being slightly larger than that in **2**, according to the results at the vanadium K-edge. The parameters which better reproduce experiments are collected in Table 2. The σ value of the third shell for **1** is larger than that for **2**, signature of a wider distribution of distances for vanadium atoms in **1** than in **2**.

Magnetic Measurements. In Figure 8 is presented the thermal variation of the magnetization for **1** and **2** ($T_C = 260$ K for **1** and 310 K for **2**). The magnetization versus magnetic field curves of **1** and **2** at 5 K are displayed in Figure 9. For compound **1**, the magnetization does not saturate; its value at highest field is around $M/N_A\mu_B$ (N_A, Avogadro constant, μ_B = Bohr magneton), $0.3\mu_B$, that is, $^1/_3$ of the $1\mu_B$ expected value for a $V_1Cr_{2/3}$ stoichiometry. These data are consistent with the presence of paramagnetic species in **1**. The coercive field is less than 50 G at 5 K. For compound **2**, at 5 K, the magnetization reaches a saturation plateau with a value of $M/N_A\mu_B = 0.98$, which is, within experimental uncertainty, the expected value

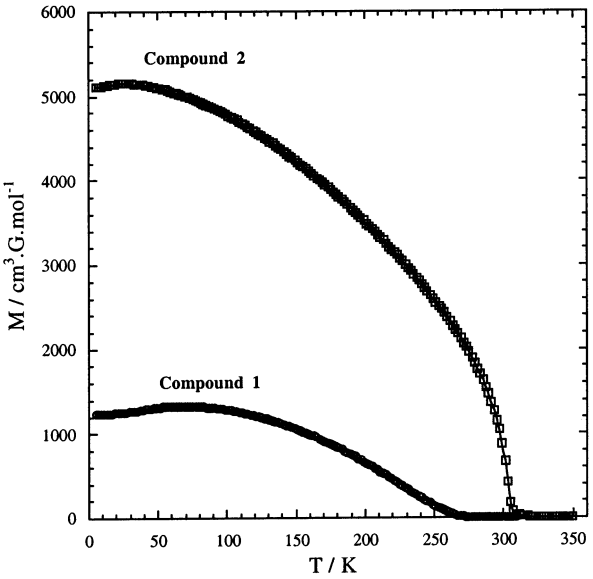

Figure 8. Thermal dependence of the magnetization of **1** (−○−) and **2** (−□−).

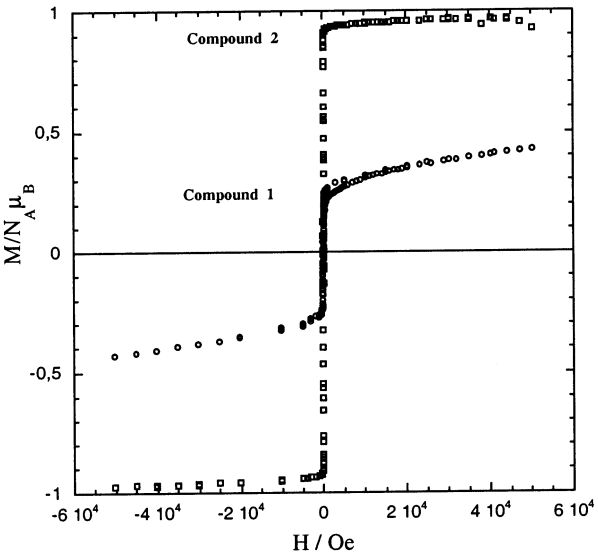

Figure 9. Field dependence of the magnetization of **1** (−○−) and **2** (−□−) at 5 K.

($1\mu_B$) for an ideal $V_1Cr_{2/3}$ composition. The coercive field is less than 50 G; compound **2** is a soft magnet. At higher temperatures, as expected, the saturation is no longer reached, because the magnetic field cannot overcome the thermal agitation.

***T*$_C$ Measurements.** We determined by permeability measurements[16] the T_C's of the VCr derivatives synthesized in the synthetic conditions described in the Experimental Section and in Table S1 with different initial V(III)/V(II) and V(II)/[Cr(CN)$_6$]$^{3-}$ ratios.

In Figure 10 is shown a plot of the Curie temperatures versus %V(III) for the compounds precipitated from solutions having different initial percentages of V(III) and a V(II)/[Cr(CN)$_6$]$^{3-}$ ratio = $^3/_2$ (series a). In the range 1−20% of V(III), the compounds present T_C around 310(±8) K. The T_C distribution is therefore less than 2.6%. For larger amounts of V(III) in solution, the T_C decreases slowly down to 296 K for 50% of V(III). Figure 10 also shows the results for the series of VCr

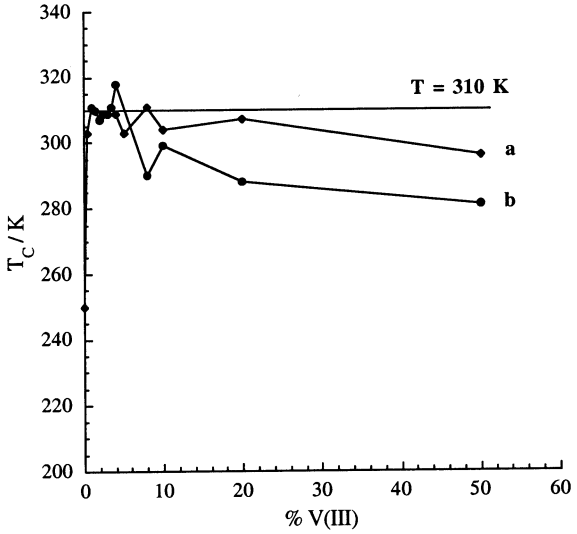

Figure 10. Curie temperatures versus percentage of V(III) in solution: (a) series a (−◆−); (b) series b (−●−).

obtained in similar conditions but with smaller V(II)/[Cr(CN)$_6$]$^{3-}$ ratios (series b). The T_C's for this later series are lower than those obtained for compounds prepared with a stoichiometric V(II)/[Cr(CN)$_6$]$^{3-}$ ratio.

Discussion

The present study was undertaken when we realized that the aqueous solution synthesis of VCr derivatives performed in anaerobic conditions (glovebox, 3 ppm O_2) [to avoid traces of V(III) or $V^{IV}O$] led, in our hands, to compounds whose T_C's lie below room temperature. This was in strong contrast with our former results obtained by the Schlenk technique (and uncontrolled amount of oxidized vanadium in solution) which lead to room-temperature magnets.[1a,6,7,9]

First, we used electronic spectroscopy to characterize aqueous solutions of V(II) and V(III) (Figure 1), and we checked that both are stable in the conditions of the synthesis of high T_C VCr derivatives:[1a,9] (i) V(II) remains unoxidized in anaerobic conditions (no change during at least 3 days); (ii) under slow diffusion of dioxygen in the solution, the oxidation of V(II) leads to V(III), and no presence of $V^{IV}O$ is observed. We then followed by electronic spectroscopy the first steps of the formation of $V_1[Cr(CN)_6]_{2/3}$ in two kinds of conditions: (a) for a mixture $V_1/Cr_{2/3}$ of V(II) and [Cr(CN)$_6$]$^{3-}$ aqueous solutions (Figure 2) and (b) for a mixture $V_1/Cr_{2/3}$ of V(II) and [Cr(CN)$_6$]$^{3-}$ aqueous solutions, in the presence of VCl_3 [molar ratio V(III)/V(II) = 4/100]. A similar reaction between a mixture V_1/Cr_1 of V(III) and [Cr(CN)$_6$]$^{3-}$ aqueous solutions was also carried out.

The main conclusions are the following: (a) The solubility of $V_1[Cr(CN)_6]_{2/3}$ is very weak. The precipitation of the blue VCr solid is observed in a few minutes from V(II) and chromicyanide solutions, even at high dilution. (b) The precipitation is much slower when chromicyanide reacts only with V(III). (c) The precipitation is faster when a small amount of V(III) is added to the V(II)/chromicyanide mixture.

The infrared spectrum of solid **1** (Figure 3) shows a band with several shoulders at 2110 cm^{-1} and below, indicating a distribution of different cyanide oscillators. For **2**, the narrower

Scheme 2

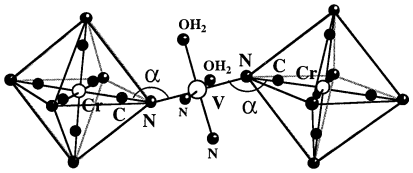

band without shoulders at 2116 cm^{-1} is in agreement with a single cyanide bridging species and previous results.[4]

The X-ray absorption spectroscopy gives clear evidence that in **1** and **2** (a) the chromicyanide ion is kept unchanged with six cyanide ligands around the chromium in an octahedral environment and then vanadium neighbors, (b) vanadium is V(II) because there are no detectable amounts of V(III) or $V^{IV}O$, as expected from the $V_1Cr_{2/3}$ stoichiometry, and (c) the V(II) ion is octahedral with four N-bonded cyanide ligands and two water molecules, always in agreement with the $V_1/Cr_{2/3}$ stoichiometry. The main differences between the EXAFS of the two compounds are essentially the V−N distances, slightly longer in **1** than in **2**, and the intensity of third shell of neighbors, which is weaker in **1** than in **2**. Keeping in mind the cubic face-centered structure of Prussian blue analogues, we find that all of these data converge on the hypothesis that the chromicyanide entities are more loosely bound in **1** and more tightly connected to vanadium(II) ions in **2** (shorter V−N distances). The Cr−C≡N−V units are well-built in **2**, presenting a C−N−V angle $\alpha = 168°$ (Scheme 2, showing the tilt of the $[Cr(CN)_6]$ octahedron, as compared to a regular face-centered cubic situation), whereas the larger Debye−Waller factors in **1** (Tables 1 and 2) express a wider distribution of angles α. In brief, **2** is better ordered than **1**.

These structural conclusions are consistent with the magnetic properties. According to Néel,[21] everything being equal, T_C is proportional to $|J|$ and Z (the number of magnetic neighbors). For **1** and **2**, Z is the same ($Z = 4$ around the vanadium), which means that $|J|$ is weaker in **1** than in **2**. The shorter vanadium−nitrogen distances and the better organization of the Cr−C≡N−V sequences in **2** induce a better overlap of the vanadium and chromium magnetic orbitals, a larger antiferromagnetic $|J|$, a higher T_C value, and the magnetization at saturation expected for the $V_1Cr_{2/3}$ composition. The saturation magnetization is no longer reached in **1**, even at low temperature, because the [Cr−C≡N] and V(II) units are not tightly connected. Part of the chromium and vanadium spins can behave independently.

Another important characteristic of **2** is that its T_C at 310 K and its magnetization at saturation remain unchanged after thermal cycles from 4 to 350 K. This result is in contrast with previous observations[4,6−10] that when cycling the temperature around T_C in $V_1Cr_{2/3}$ compounds with an initial high T_C (i.e., $T_C > 330$ K), the final stable T_C decreases. If one considers the VCr derivatives presenting such unstable T_C's as metastable derivatives, the compounds obtained in the presence of V(III) can be called "thermodynamical" compounds. The structural model with $\alpha = 168°$ given in Scheme 2 allows for a straightforward explanation of the higher T_C's of the metastable samples; they present a (metastable) structure with α angles closer to 180° (corresponding to weaker tilt of the $[Cr(CN)_6]$ octahedron) and therefore larger orbital overlaps, $|J|$, and T_C's. Heating the sample and cycling the temperature bring the system to the stable structure with the α angles closer to 168°. It is particularly significant that the stable $T_C = 310$ K value, reached here directly, corresponds exactly to that found by Girolami for a compound of the same stoichiometry synthesized by the sol−gel approach after cycling the temperature around T_C.[22]

Therefore, the presence of vanadium(III) during the synthesis of the VCr derivatives has a clear influence on the structure and on the magnetic properties of the derivatives and cannot be underestimated. The vanadium(III) is not present in the solid state but is observed in solution after reaction. The minimum amount of V(III) necessary to lead to a room-temperature magnet is around 1%. The two observations point out a catalytic role of V(III) ion in the formation of the solids. We propose below a reaction scheme, summarizing the different experimental observations:

$$V^{3+}(aq) + n[Cr(CN)_6]^{3-}(aq) \rightarrow [V^{3+}(-NC-Cr(CN)_5)_n]^{3(n-1)-}(aq) \quad (1)$$

$$[V^{3+}(-NC-Cr(CN)_5)_n]^{3(n-1)-}(aq) + V^{2+}(aq) \rightarrow [V^{2+}(-NC-Cr(CN)_5)_n]^{(3n-2)-}(aq) + V^{3+}(aq) \quad (2)$$

$$[V^{2+}(-NC-Cr(CN)_5)_n]^{(3n-2)-}(aq) \rightarrow [V(-NC-Cr)_{2/3}]^{0}\downarrow \quad \text{(precipitate when } n \approx {}^2/_3) \quad (3)$$

In step 1, V(III) ions, which are present in small amounts in solution, react with $[Cr(CN)_6]^{3-}$ to give a soluble charged species (the expected neutral entity $\{V(III)[Cr(CN)_6]\}^0$ was never observed as a precipitate). The higher reactivity of V(III) with $[Cr(CN)_6]^{3-}$, as compared to V(II), can be understood from an electrostatic argument (a trivalent species V^{3+} is better attracted than a bivalent V^{2+} one by the anionic trivalent $[Cr(CN)_6]^{3-}$) and from an electronic one; the V(II) ion, d^3 configuration, is more inert (water exchange constant, $k_{ex}(273\ K)/s^{-1} = 8.7 \times 10^1$),[23] than V(III), d^2 (water exchange constant, $k_{ex}(273\ K)/s^{-1} = 5 \times 10^2$).[24]

In step 2, V(II) ions, present in large concentration in solution, interact with the anionic $[V^{3+}(-NC-Cr(CN)_5)_n]^{3(n-1)-}$ entities, and an electronic transfer between V(II) and V(III) occurs.[25] The redox process can occur because in the soluble {V(III)−NC−Cr} units the V(III) d orbitals (t_{2g} symmetry) are stabilized by the ligand field created by the N-bonded cyanide ligands (interaction with the empty π^* orbitals), as compared to the hexa-aqua situation, and V(III) becomes more reducible. The $V^{2+}(aq)/V^{3+}(aq)$ couple presents a standard redox potential $E° = -0.255$ V[26] with a self-exchange rate constant, $k_{AA}(mol^{-1}$

(21) Néel, L. *Ann. Phys. (Paris)* **1948**, *3*, 137−198.

(22) It is also the case for the sample prepared with 4% of V(III) (and some excess of chromicyanide) which presents the highest T_C (318 K) in the series and a $V_1Cr_{2/3}$ stoichiometry − see Figure 10. When heated to 350 K, its T_C decreases then down to 313 K. Slight differences in the reproducibility of experimental synthetic conditions are the only hypotheses that we can propose to explain for obtaining this compound with the highest T_C in the series and its metastability.

(23) Ducommun, Y.; Zbinden, D.; Merbach, A. E. *Helv. Chim. Acta* **1982**, *65*, 1385−1390.

(24) Hugi, A. D.; Helm, L.; Merbach, A. E. *Helv. Chim. Acta* **1985**, *68*, 508−521.

(25) *Reaction Mechanisms of Inorganic and Organometallic Systems*; Jordan, R. B., Ed.; Oxford University Press: New York, 1991; pp 167−197 and references therein.

(26) Creaser, I. I.; Sargeson, A. M.; Zanella, A. W. *Inorg. Chem.* **1983**, *22*, 4022.

$s^{-1}) = 10^{-2}$,[27] smaller than the rate of ligand substitution. Thus, here, an outer-sphere electron-transfer V^{2+} (aq)/$V^{3+}(NC)_n$ can be expected to be present and to be the limiting step.

In any case, step 2 provides soluble V(II)−Cr entities $[V^{2+}(-NC-Cr(CN)_5)_n]^{(3n-2)-}$ (aq), with well-designed V(II)−NC−Cr(III) bridges, whereas the V(III) (aq) ions regenerated in solution are able to react once more with other $[Cr(CN)_6]^{3-}$ in recurring steps 1 and 2. The repeated catalytic sequence of steps 1 and 2 progressively increases the concentration (and/or) size of well-built $[V^{2+}(-NC-Cr(CN)_5)_n]^{(3n-2)-}$ (aq) entities, and, in step 3, the neutral $\{V(II)[Cr(CN)_6]_{0.67}\}^0$, whose solubility is very low, precipitates, displacing the equilibrium toward a total precipitation, V(III) remaining in solution.

One final remark will deal with the syntheses carried out with smaller V(II)/$[Cr(CN)_6]^{3-}$ ratios or with large amounts of V(III) which lead to products presenting lower T_C's. These compounds present stoichiometries different from $V_1Cr_{2/3}$ and no alkali cations (elemental analysis), in agreement with the presence of V(III) in the solid, confirmed by the X-ray absorption spectrum at the K-edge of vanadium. The larger the percentage of V(III) in solution is (above 20%), the larger the amount of V(III) is in the final solid. In both cases, the presence of V(III) weakens the $|J|$ value and decreases T_C.

Conclusions

We proposed in this paper a new synthetic approach to high T_C VCr Prussian blue analogues; small amounts of V(III) during the synthesis lead to derivatives which display a stoichiometry close to the $V_1Cr_{2/3}$ ideal one. The solids are free from V(III). Their structure is made of $[Cr(III)CN)_6]$ units linked to octahedral vanadium(II) ions by bent C−N−V units (168°). The observed magnetization fits well with the $V_1Cr_{2/3}$ stoichiometry. The Curie temperatures obtained in this way are not the highest obtained so far, but they are reproducible and remain constant after heating the samples above T_C. The tilted configuration of the $[Cr(III)CN)_6]$ octahedron, with a C−N−V angle $\approx$ 168°, reminiscent of the situation in some distorted perovskites, is therefore a thermodynamically stable one. The higher but unstable T_C's sometimes observed in derivatives with identical $V_1Cr_{2/3}$ stoichiometry are easily explained by metastable structures with C−N−V angles > 168°, corresponding to less tilted configurations of the $[Cr(III)CN)_6]$ blocks. The key role of V(III) can be also demonstrated in the synthesis of VCr Prussian blue analogues, where the stoichiometry is varied by inserting alkali cations (K, Rb, Cs).

Acknowledgment. We would like to thank Dr. F. Tournilhac for permeability measurements, the European Community for a Marie Curie Grant (R.G.) and TMR support (ERBFMBICT972644 and FMRXCT980181), and CNRS for a temporary position (R.G.).

Supporting Information Available: Synthetic procedure, elementary analysis, T_C's and IR data and a table summarizing the data of compounds **1S**−**23S**, the electronic spectra of a $V(SO_3CF_3)_3$ and $(TBA)_3[Cr(CN)_6]$ solution mixture, the chromium K-edge spectra of compounds **1**, **2**, and $K_3[Cr(CN)_6]$, the magnetization versus field curves of **1** and **2** at different temperatures, and the Fourier transform moduli and imaginary parts of the EXAFS signal at the vanadium K-edge for **1**, **2**, and model (PDF). This material is available free of charge via the Internet at http://pubs.acs.org.

JA020528Z

(27) Chou, M.; Creutz, C.; Sutin, N. *J. Am. Chem. Soc*. **1977**, *99*, 5615.